MANAS Journal of Engineering
ISSN 1694-7398 | e-ISSN 1694-7398

Volume 10, Issue 1, (2022) Pages 21-34
https://doi.org/10.51354/mjen. 943729

Structural and compressibility properties of weft-knitted rib fabrics from glass yarn

Mehmet Erdem İnce

Gaziantep University, Engineering Faculty, Textile Engineering Department, 27310 Gaziantep, Turkey
einceg@gantep.edu.tr, meince@ncsu.edu, ORCID: 0000-0001-7537-9172

ABSTRACT

The structural and compressibility properties of the weft-knitted glass yarn fabrics from 1x1, 2x2, English, and fisherman rib architectures were investigated in this study. Due to their tight structures; 2x2 and fisherman rib fabric architectures exhibited higher loop density, and shorter loop length than 1x1 and English rib fabric architectures. English and fisherman rib fabric architectures displayed higher fiber volume fraction than 1x1 and 2x2 rib architectures in multi-layer compaction and recovery tests where the pressure was varied between 2 and 200 kPa. Number of layer increased the fiber content that pointed the nesting between the fabric layers. As a result of lack of complete recovery from compression; the fabrics exhibited lower thicknesses (i.e. higher fiber volume fractions) during the recovery periods than they did during the compression periods. A second order polynomial regression model with 0,89 R^2 (coefficient of determination) was developed to estimate the fiber volume fraction by means of knit architecture, number of fabric layers, pressure, and measurement period.

ARTICLE INFO

Research article

Received: 27.05.2021
Accepted: 7.04.2022

Keywords:
Glass yarn,
weft-knitted fabric,
fabric structural properties,
fabric compressibility

**Corresponding author*

1 Introduction

Due to their better specific strength, impact resistance, and non-corrosible features than the conventional materials; the use of fiber reinforced polymers (FRPs) is increasing in all segments of industrial areas ranging from automotive to marine, aerospace, and defense. FRPs principally consist of two constituents – fiber and polymeric resin – while the low density resin surrounding the fibers protects them from severe environmental conditions and transfers the applied load on to them; high performance fiber improves mechanical properties of the integrated body. The mechanical properties of FRPs for a given direction are controlled by the relative amount (volume fraction) of fibers lying in that direction. This makes the FRPs designable depending on the forces applied during their use [1, 2].

Fiber volume fraction (FVF) of a FRP is a function of the reinforcement's structural and compressibility properties. Therefore, measuring the reinforcement fabric's response in compression and relaxation periods plays a critical role to predict the FVF of the composite product. The compaction behaviour of the reinforcement is also central to design a firm mold and to estimate the mold filling time [3-5]. This study is about the structural properties and compaction behaviors of glass yarn weft knit fabrics and the relevant studies are given in the following paragraphs.

Pearce and Summerscales [6] studied compaction behaviour of plain woven glass fabrics, where one-layer fabric displayed higher fiber content than multi-layer fabrics. While lack of nesting was observed between layers, the fiber content was increased by the repeated compaction. Lekakou, Johari and Bader [7] developed a nonlinear elastic compaction model and confirmed it with the liquid molding of layered 2D plain woven glass fabrics. The number of fabric layers decreased the in-plane resin flow permeability, which pointed out the inter-layer nesting.

Robitaille and Gauvin [8] reviewed the studies about the compaction and relaxation of glass fiber nonwoven and woven fabrics. The researchers reported that while both the number of layers and number of compaction cycles increased the stiffness (compaction resistance), only the number of cycles improved the fiber content due to lack of nesting between layers. Luo and Verpoest [9] measured the compactions of a multi-layer fabric (a plain weft-knitted glass fabric was sewn between two plies of random glass mats), its constituents, and a 2D plain woven glass fabric. The number of layers improved the fiber content of the plain knitted fabric that was associated with the interlocked loopy fabric structure allowing nesting.

Potluri and Sagar [10] developed an energy-minimization-based compaction model considering the compression and bending of the yarn, and confirmed it via 2D and 3D woven

glass fabrics. The researchers measured the nesting for 2D fabric and obtained good agreement between the model and the practice. Lomov and Molnár [11] studied the existence of nanofiber interleaves on the compaction of 2D plain woven carbon fiber fabrics. The scientists stated that successive compaction cycles improved the fiber content through increasing the stiffness of the stack, and both fabric stacks with/without nanofiber exhibited the nesting.

Yousaf, Potluri and Withers [12] examined the influence of pattern (plain, twill and sateen) and the number of layers on the compression of 2D woven glass fabrics. Due to its tight and less bendable structure, the plain woven fabric exhibited the highest compaction resistance. While all weave patterns displayed nesting, the plain weave showed the highest nesting that was attributed to its shorter yarn float length.

Due to its low cost, flexible, and fast production; the use of weft-knitting in composite industry is growing. Easily stretchable and formable weft knit fabrics make it possible to produce complex and seamless 2D or 3D preforms in one step. Because of their 3D form loops and porous structure allowing nesting, the composites reinforced by weft knit fabrics show improved impact resistance as compared with the other textile fabrics.

However, due to their loose structure and low load-carrying capability caused by low fiber content with lack of fiber directionality; weft-knitted fabrics are disadvantageous for in-plane strengthening [13–16]. This disadvantage of the weft knit fabrics makes their compaction critical. However, no particular attention was paid to the compaction of glass yarn weft knitted fabrics with various architectures in the literature. Focus in previous studies was mostly directed to the compaction of commercially available mat and woven fabrics. We hypothesized that the compaction of glass yarn weft knit fabrics yarn can be controlled by knit architecture and number of fabric layers.

2. Materıal and methods

The three-ply E-glass multi-filament yarn with a single-ply yarn count of 136 tex and fiber diameter of 9 microns was used to produce fabrics on the Brother KH-864 flat, weft knitting machine with 5 gauge fineness. Table 1 shows the experimental plan. Figure 1 illustrates technical notations and hand-drawn views of the weft knit fabrics; Figure 2 shows the simulations of the knits from filament yarn; and Figure 3 displays the real pictures of the knit fabrics, both under tension on the knitting machine and on the bench in stress-free form.

Table 1. *Experimental study plan*

Variable:	Knit architecture	Number of fabric layer	Measurement period	Pressure [kPa]
Levels:	1x1 rib 2x2 rib English rib Fisherman rib	1 2 3	compression recovery	2 - 200

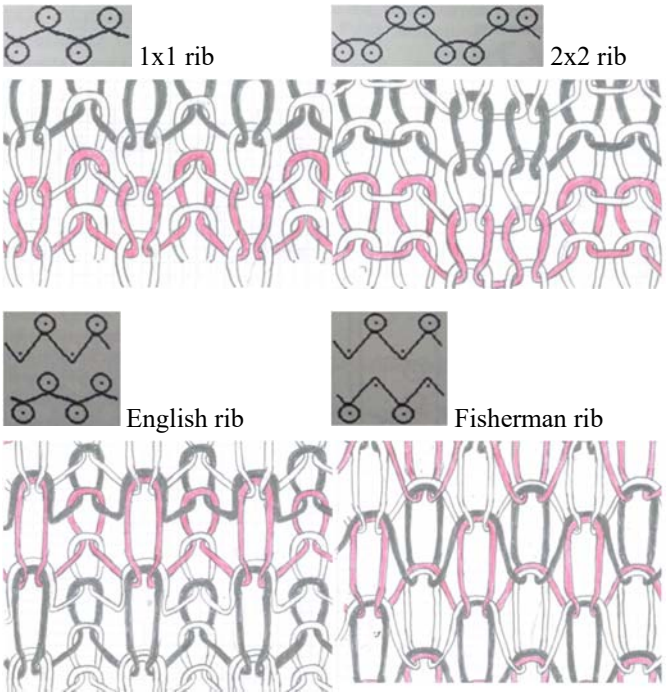

Figure 1. *Technical notations [17, 18] and hand-drawn views of the knit architectures*

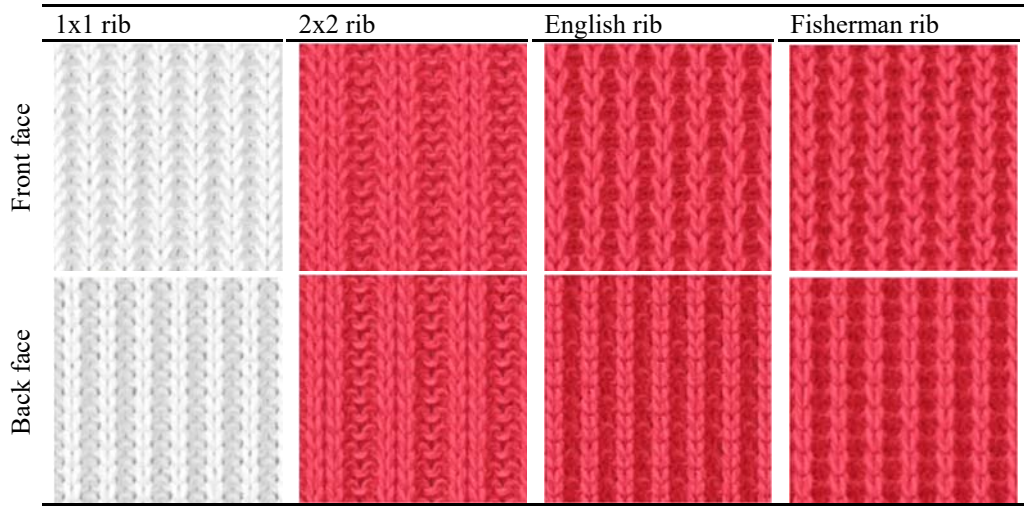

Figure 2. *The simulations of the knit architectures from filament yarn*

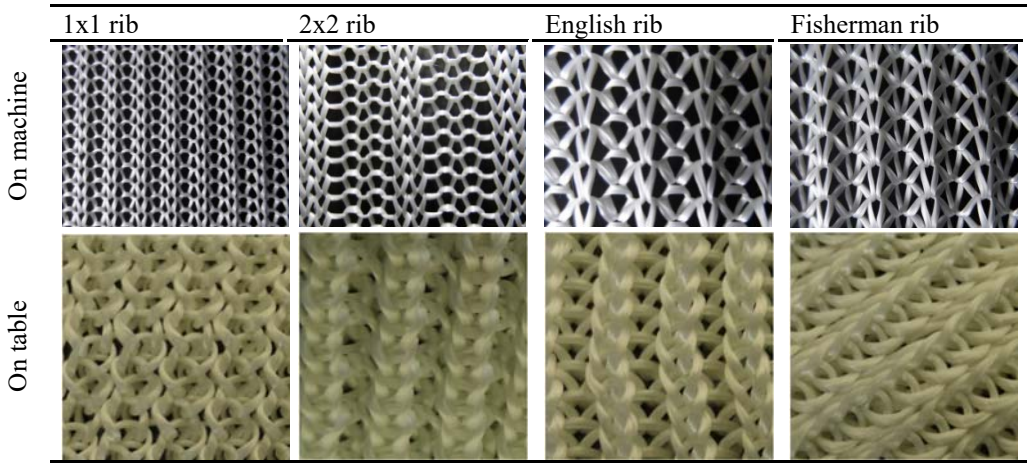

Figure 3. *Real pictures of the knit architectures*

2.1. Measurement of physical and structural properties of single-layer fabrics

2.1.1. Thickness

The digital thickness gauge (Figure 4) was used to measure the thicknesses of the fabrics. The gauge has gradually-increased weights to apply pressures from 2 to 200 kPa. Thicknesses measured under 200 kPa were utilized for the thickness and fiber content analyses of the one-layer fabrics.

Figure 4. *The thickness gauge and its additional weights*

2.1.2. Areal density

The weights of 5x5 cm^2 single-layer pieces cut from fabrics by a special die cutter were measured in line with ASTM D3776 [19]. The fiber volume percent were calculated using the thickness (measured under 200 kPa pressure) and the areal density along with Equation 1 where A_f, ρ_f , t are fabric areal density, fiber volumetric density, and fabric thickness, respectively. Glass fiber material density was assumed to be 2,5 g/cm^3.

$$Fiber\ volume\ percent\ [\%] = \frac{A_f}{\rho_f * t} * 100 \qquad (1)$$

2.1.3. Course density, wale density, and loop length

ASTM D8007 [20] was followed to determine the course and wale densities. The loop density (number of loops for every centimeter square) was calculated from the product of the relevant course and wale densities. The loop length was measured according to BS 5441 [21].

2.2. Measurement of the thickness of single and multi-layer fabrics

Knitted fabrics (in single-, or multi-layer form) were placed on the anvil of the digital thickness gauge (Figure 4). The presser foot with compaction pressure of 2 kPa was lowered onto the fabric. After at least 30-second wait, once the gauge's display became invariant, the thickness was recorded. Thereafter, extra masses were sequentially added on the presser foot. After the adding of each mass, at least 30 seconds was waited to record the thickness on the steady screen of the thickness gauge. When the compaction was terminated at 200 kPa, the masses on the presser foot were removed sequentially and the relaxation thickness for each removal was recorded. The each measured thickness was converted into fiber volume percent using Equation 2 where n, A_f, ρ_f, t are number of fabric layers, average areal density of single-layer fabric, fiber volumetric density, and fabric stack thickness, respectively. A trial form of the Jump® [22] software was used for drawing graphs and analysis.

$$Fiber\ volume\ percent\ [\%] = \frac{n * A_f}{\rho_f * t} * 100 \qquad (2)$$

3. Results and discussion

3.1. Physical and structural properties of single-layer fabrics

3.1.1. Thickness, areal density, and fiber volume percent

Tuck stitches contracted English and fisherman ribs in both width and length direction and increased their thickness (Figure 5 and Table 2). Similarly, the number and position of the tuck stitches in single-bed cotton yarn weft knit fabrics significantly affected the properties of the fabric and the tuck stitch increased the fabric thickness and areal density in the previous studies [23-25]. İnce and Yıldırım [26] also observed that the tuck stitch increased the thickness and areal density in single-bed glass yarn weft knit fabrics because of left to right turning and nesting of the loop bars.

On the other hand, the successive placement of binary face and back plain loop bars increased the internal tension that dramatically narrowed the knit architecture of 2x2 rib in the course direction after removal from the machine. Thus, due to shortening in the fabric width direction, 2x2 rib exhibited higher thickness than 1x1 rib. Pairwise comparisons showed that the thickness difference between fisherman and 2x2 ribs did not reach a statistically significant level, as was the difference between English and 1x1 ribs. The low internal stress resulting from the architecture revealed a loose knit structure for the 1x1 rib fabric that exhibited the lowest thickness. Parallel results were detected for the influences of knit architecture on areal density and fiber volume percent. The 2x2 rib knit architecture and the architectures incorporating tuck stitches showed higher areal density and fiber content than 1x1 rib.

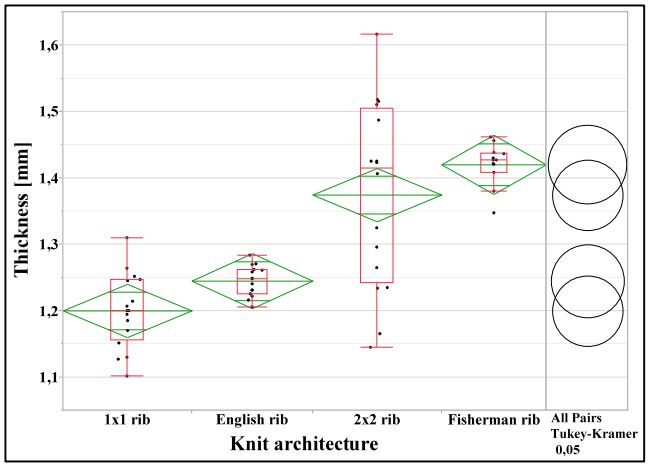

a

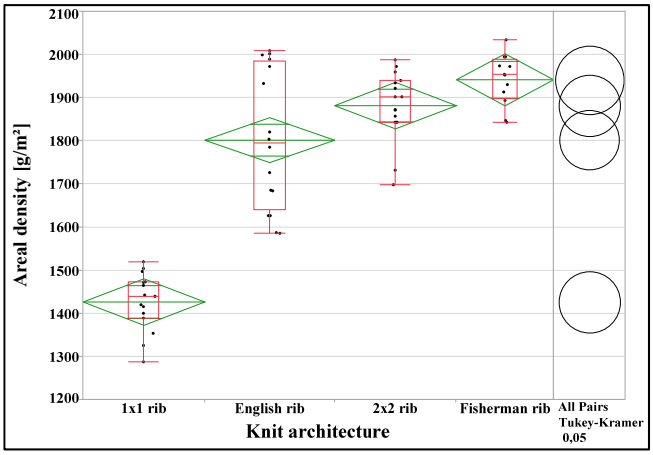

b

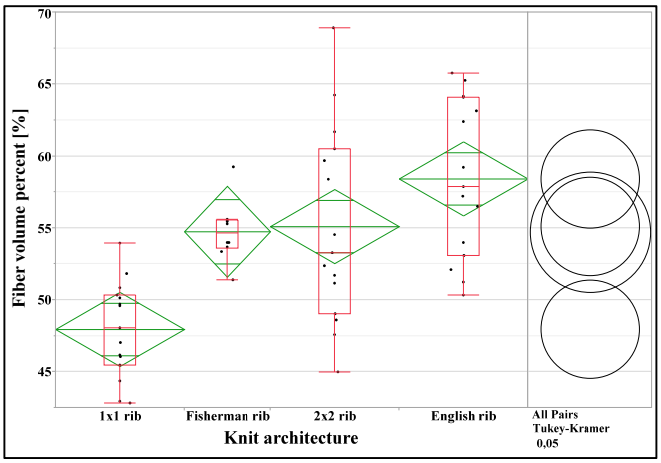

c

Figure 5. *The effect of knit architecture on thickness (a), areal density (b) and fiber volume percent (c)*

Note: The space between the upper and lower corners of the green parallelogram represents the 95% confidence interval. One comparison circle is given in the right-hand column for the mean of each knit architecture level. Comparison circles representing significantly different means are either non-intersecting or slightly intersecting.

Table 2. *The effect of knit architecture on thickness, areal density and fiber volume percent*

Property	Knit architecture				n	mean	sd	LL	UL	p-value
Thickness [mm]	Fisherman rib	A			13	1,42	0,03	1,40	1,44	< 0,0001
	2x2 rib	A			16	1,37	0,14	1,30	1,45	
	English rib		B		15	1,24	0,02	1,23	1,26	
	1x1 rib		B		16	1,20	0,06	1,17	1,23	
Areal density [g/m^2]	Fisherman rib	A			12	1941,78	59,18	1904,2	1979,4	< 0,0001
	2x2 rib	A	B		15	1881,99	82,08	1836,5	1927,4	
	English rib		B		16	1801,83	161,47	1715,8	1887,9	
	1x1 rib			C	15	1426,46	66,99	1389,4	1463,6	
Fiber volume percent [%]	English rib	A			15	58,41	5,45	55,40	61,43	< 0,0001
	2x2 rib	A			15	55,10	6,84	51,31	58,88	
	Fisherman rib	A			10	54,74	2,05	53,27	56,21	
	1x1 rib		B		15	47,94	3,31	46,11	49,78	

Note: Levels not united with the same alphabetical capital letter are significantly different (α = 0,05). **n**: number of measurements, **sd**: standard deviation, **LL**: lower limit, **UL**: upper limit. The limits are based on a 95% confidence level. p-values less than 0,05 are indicative of statistical significance and are red.

3.1.2. Course-, wale-, and loop-density

The knit architecture played a statistically significant role on course-, wale-, and loop-density; and the knit architecture of 2x2 ribs overwhelmed the other architectures in terms of these densities (Figure 6, Table 3). The fabric with 2x2 rib architecture showed a dramatic contraction in the course direction that increased the fabric's tightness. After removal of the fabric from the machine, the tuck stitches on both faces of the fisherman rib fabric rotated the loop bars in clockwise direction (Figure 3). As a result of this rotation, the loop bars nested under each other that increased the loop density of the fisherman rib fabric. On the other hand, because of its loose structure with less internal tension, 1x1 rib fabric showed the lowest loop density.

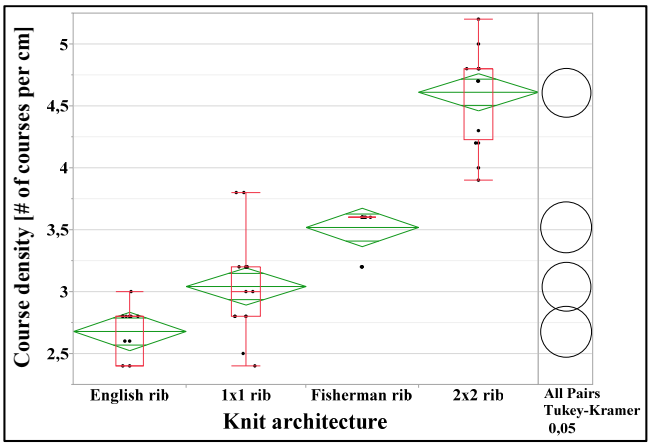

a

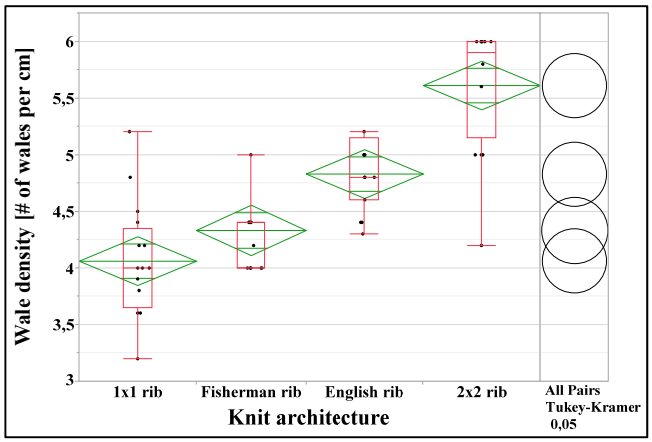

b

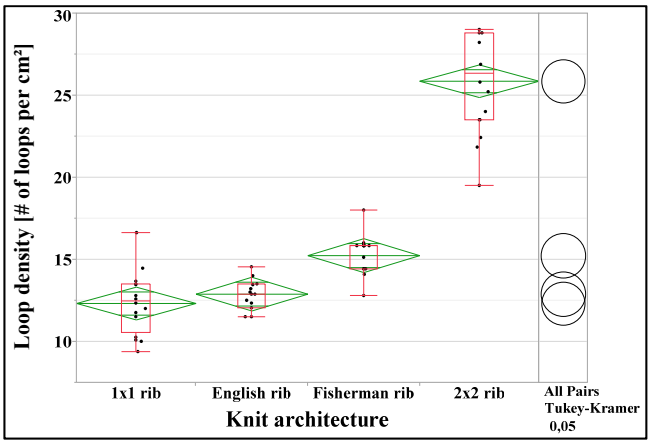

c

Figure 6. *The effects of knit architecture on course- (a), wale- (b), and loop-density (c)*

Table 3. *The effects of knit architecture on course-, wale-, and loop-density*

Property	Knit architecture				n	mean	sd	LL	UL	p-value
Course density [#/cm]	2x2 rib	A			16	4,61	0,37	4,41	4,81	< 0,0001
	Fisherman rib		B		15	3,52	0,17	3,43	3,61	
	1x1 rib			C	16	3,04	0,38	2,84	3,25	
	English rib				D	15	2,68	0,20	2,57	2,79
Wale density [#/cm]	2x2 rib	A			16	5,61	0,54	5,32	5,90	< 0,0001
	English rib		B		16	4,83	0,30	4,67	4,99	
	Fisherman rib			C	15	4,33	0,33	4,15	4,51	
	1x1 rib			C	16	4,06	0,50	3,80	4,33	
Loop density [#/cm²]	2x2 rib	A			16	25,86	3,09	24,22	27,51	< 0,0001
	Fisherman rib		B		15	15,24	1,21	14,57	15,91	
	English rib			C	15	12,90	1,02	12,33	13,46	
	1x1 rib			C	16	12,32	1,88	11,32	13,32	

3.1.3 Loop length

Among many structural parameters, the loop length is the most effective one that controls the properties of the knitted fabric. The shorter the loop length, the tighter (more compact) the fabric is. The knit architecture showed a statistically significant effect on the loop length (Figures 7, and Table 4). While the 1x1 rib fabric exhibited the longest loop length, the fisherman rib demonstrated the shortest one. The presence of tuck stitches in English and fisherman ribs, and the shrinkage in the direction of knitting line in 2x2 rib decreased the loop length.

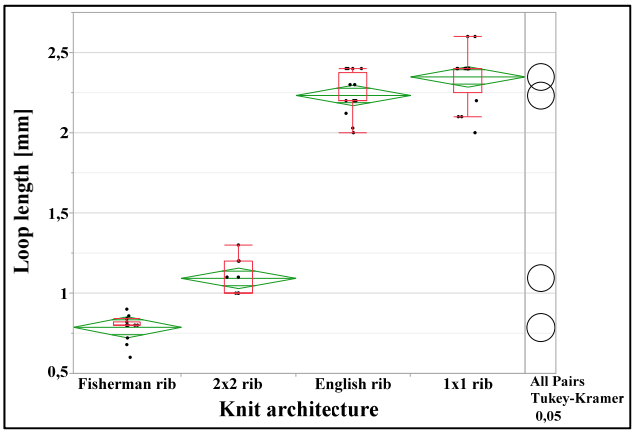

Figure 7. *The effects of knit architecture on loop length*

Table 4. *The effects of knit architecture on loop length*

	Knit architecture				n	mean	sd	LL	UL	p-value
Loop length [mm]	1x1 rib	A			16	2,35	0,17	2,26	2,44	< 0,0001
	English rib	A			16	2,23	0,13	2,17	2,30	
	2x2 rib		B		16	1,09	0,12	1,03	1,16	
	Fisherman rib			C	15	0,79	0,07	0,75	0,83	

3.2. Thickness analysis based on multi-layer fabric thickness measurement

3.2.1. The effect of knit architecture on thickness

The 2x2 rib fabric displayed the highest thickness, while 1x1 rib fabric showed the lowest one (Figure 8 and Table 5). The only statistically significant difference in thickness was observed between 1x1 and 2x2 rib fabrics. The thickness difference between the other knit architectures could not reach a statistically significant level (α = 0,05). These findings are in line with the analysis of the influence of knit architecture on the thickness of single-layer fabrics, which was measured under 200 kPa compaction pressure (Figure 5-a, Table 2).

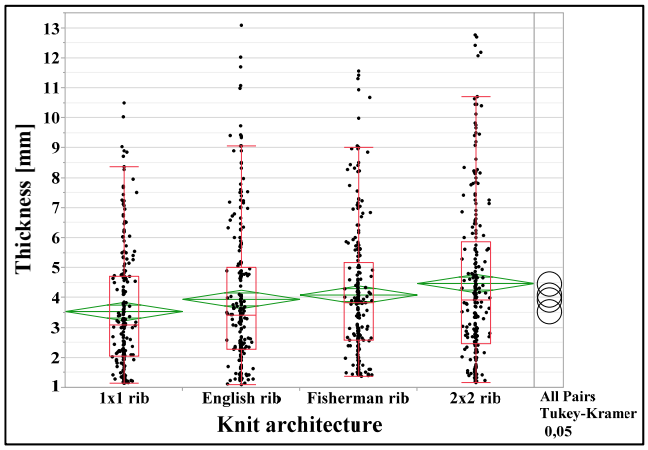

Figure 8. *The effect of knit architecture on single- and multi-layer fabric thicknesses*

Table 5. *The effect of knit architecture on single- and multi-layer fabric thicknesses*

Property	Knit architecture			n	mean	sd	LL	UL	p-value
Thickness [mm]	2x2 rib	A		225	4,48	2,66	4,13	4,82	0,0004
	Fisherman rib	A	B	225	4,09	2,23	3,80	4,38	
	English rib	A	B	225	3,95	2,42	3,63	4,27	
	1x1 rib		B	225	3,54	2,01	3,28	3,80	

3.2.2. The effect of knit architecture on fiber content

Fisherman rib knit architecture exhibited the highest fiber volume percent, while 1x1 rib knit architecture showed the lowest one (Figure 9 and Table 6). Significant fiber content change (α = 0,05) was only observed between fisherman and 1x1 rib architectures. The tuck stitches narrowed the fabric in both width and length direction that formed a compact and tight fabric structure. In 2x2 rib knit fabric architecture: the side-by-side placement of binary face and back loop bars increased the fabric internal tension in the course direction. After removal of the fabric from the machine; this inner pull shrank the fabric in the course direction, and thus increased the tightness of the fabric. These findings agreed with the Figure 5-c, Table 2 where the influence of knit architecture on the fiber volume percent of single-layer fabrics under 200 kPa compaction pressure was displayed.

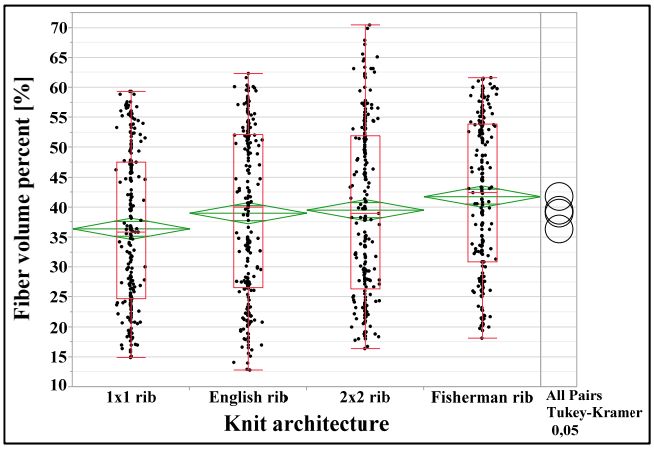

Figure 9. *The effect of knit architecture on fiber volume percent*

Table 6. *The effect of knit architecture on fiber volume percent*

Property	Knit architecture			n	mean	sd	LL	UL	p-value
Fiber volume percent [%]	Fisherman rib	A		225	41,79	12,66	40,13	43,46	**0,0005**
	2x2 rib	A	B	225	39,54	14,37	37,65	41,43	
	English rib	A	B	225	39,03	14,16	37,16	40,89	
	1x1 rib		B	225	36,42	12,75	34,75	38,10	

3.2.3. The effect of the number of fabric layers on the normalized thickness and fiber volume percent

The number of fabric layers decreased the normalized thickness (Figure 10-a, and Table 7). Although this decrease did not reach a statistically significant level, it proved the nesting tendency in compacted multi-layer weft-knitted fabrics. On the other hand, the number of fabric layers increased the fiber volume percent at a statistically significant level (Figure 10-b and Table 7). This result, parallel with Luo and Verpoest's study [9] where the nesting was observed for the weft-knitted glass yarn plain fabric, also proved the nesting in weft-knitted glass yarn rib fabrics with various architectures. The stretchable and flexible weft knitted fabrics from 3D, porous and intertwined loops exhibit higher nesting tendency than woven and random mat fabrics. Lack of important difference (α = 0,05) was detected between 3-layer fabrics with single- and 2-layer fabrics in terms of fiber content. However, the 2-layer fabric exhibited significantly greater fiber volume percent than the one-layer fabric.

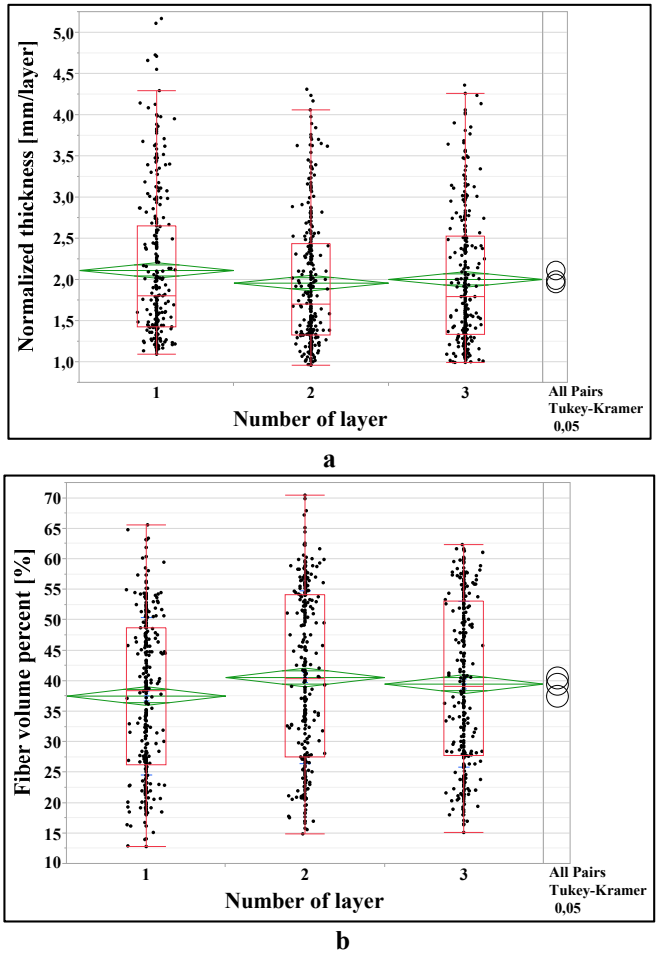

Figure 10. *The effects of the number of fabric layers on normalized thickness (a) and fiber volume percent (b)*

Table 7. *The effects of the number of fabric layers on normalized thickness and fiber volume percent*

Property	Number of layer			n	mean	sd	LL	UL	p-value
Normalized thickness [mm/layer]	1	A		300	2,11	0,88	2,01	2,21	0,0654
	3	A		300	2,00	0,80	1,91	2,10	
	2	A		300	1,96	0,80	1,87	2,05	
Fiber volume percent [%]	2	A		300	40,57	14,18	38,96	42,18	**0,0210**
	3	A	B	300	39,48	13,60	37,94	41,03	
	1		B	300	37,52	12,92	36,06	38,99	

3.2.4. The effect of force type (compression or recovery period) on thickness and fiber content

Because the first compaction crushed and repositioned the fibers in the fabric stacks, the stacks exhibited lower thickness during the subsequent recovery (relaxation) period (Figure 11-a and Table 8). Lower thicknesses in the recovery periods increased the fiber volume percent calculated in these periods.

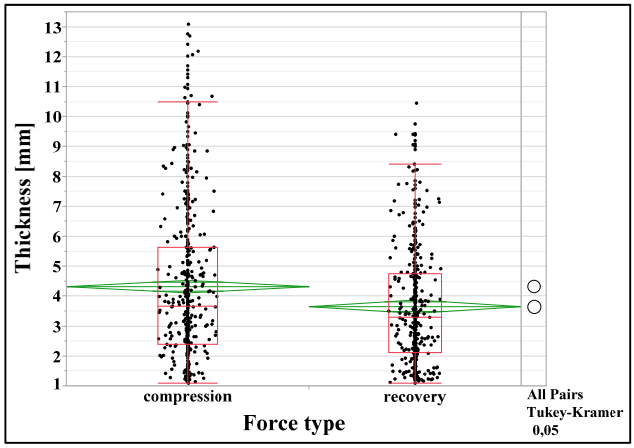

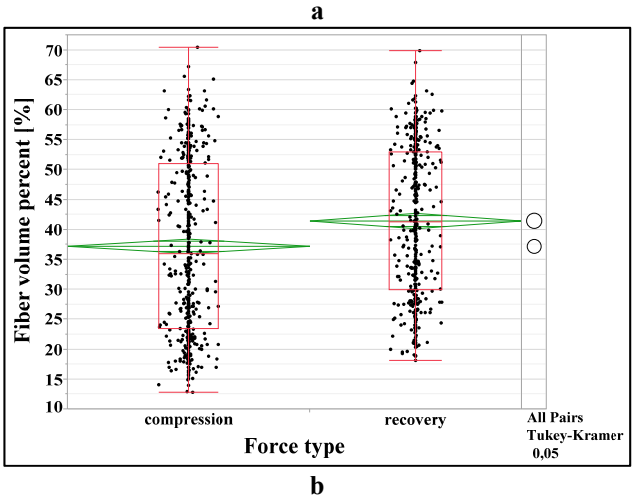

Figure 11. *The effect of measurement period on thickness (a) and fiber content (b)*

Table 8. *The effect of measurement period on thickness and fiber content*

Property	Measurement period		n	mean	sd	LL	UL	p-value
Thickness [mm]	compression	A	480	4,33	2,61	4,09	4,56	< 0,0001
	recovery	B	420	3,66	1,99	3,47	3,85	
Fiber volume percent [%]	recovery	A	420	41,44	12,49	40,24	42,64	< 0,0001
	compression	B	480	37,23	14,26	35,95	38,51	

3.2.5. The effect of pressure on fiber content

Figure 12 shows the relationship (grouped by compression and recovery periods) between pressure and fiber volume percent. The effect of pressure on the fiber volume percent exhibited a power-law character. The fiber volume percent increased vertically in the initial pressure steps then slowed down and evolved into a plateau in the higher pressure steps. Due to crushing and stiffening effect of the initial compaction, the recovery curve exhibited a higher fiber content than the compression curve did. This result was consistent with the previous studies [6, 8, 11] indicating that repeated relaxation and reloading to maximum compaction increased the rigidity and the fiber content of the fabric stack. The power law equations developed for the overall compression and recovery curves plotted in Figure 12 are given below.

General compression behaviour (R^2: 0,92; p-value < 0,0001):

$$Fiber\ volume\ percent\ [\%] = 14{,}94 * (Pressure\ [kPa])^{0{,}25} \quad (3)$$

General recovery behaviour (R^2: 0,90; p-value < 0,0001):

$$Fiber\ volume\ percent\ [\%] = 21{,}00 * (Pressure\ [kPa])^{0{,}21} \quad (4)$$

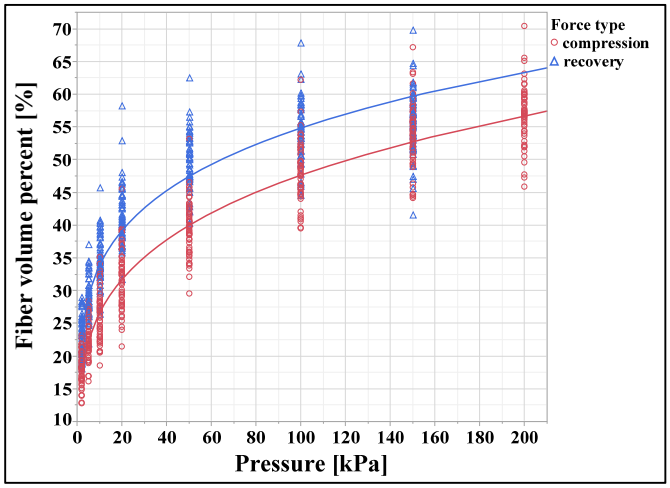

Figure 12. *The effect of pressure on fiber volume percent*

3.2.6. Development of fiber volume percent estimation equation

A regression equation was developed 1) to estimate the fiber volume percent using experimental study plan input variables and 2) to illustrate in detail how the fiber volume percent is influenced by the input variables. Among the various options, the second degree polynomial model resulted in the highest R^2 (0,888 i.e. 88,8% of the total variation in the fiber volume percent results was explained by the model) and the residuals with a nearly normal distribution. The ANOVA test for the model resulted in a p-value of less than 0,0001 that indicated the significance of the model. The black dots given in Figure 13-a were as close as possible to the linear red continuous line with the slope of one and the black dots given in Figure 13-b were almost symmetrically distributed on both sides of the blue dashed horizontal zero line. All these reinforced the reliability of the developed model. The model residuals showed a nearly normal (p = 0,0376) distribution (Figure 13-c). Equation 5 shows the developed estimation equation. All the inputs and their coefficients given in Equation 5 were statistically significant (p-values less than 0,05).

$$
\begin{aligned}
&\textit{Fiber volume percent}\ [\%] \\
&= 28{,}13 \\
&+ \textit{Match}(\textit{Knit architecture}) \begin{pmatrix} 1x1\ rib & \Rightarrow & -3{,}49 \\ 2x2\ rib & \Rightarrow & -0{,}95 \\ \textit{Fisherman rib} & \Rightarrow & 1{,}84 \\ \textit{English rib} & \Rightarrow & 2{,}59 \end{pmatrix} \\
&+ \textit{Match}(\textit{Number of layer}) \begin{pmatrix} 1 & \Rightarrow & 0 \\ 2 & \Rightarrow & 2{,}98 \\ 3 & \Rightarrow & 1{,}98 \end{pmatrix} \\
&+ \textit{Match}(\textit{Force type}) \begin{pmatrix} \textit{compression} & \Rightarrow & -3{,}28 \\ \textit{recovery} & \Rightarrow & 3{,}28 \end{pmatrix} + 0{,}27 \\
&* (\textit{Pressure}\ [kPa]) + (\textit{Pressure}\ [kPa] - 58{,}31) \\
&* (\textit{Pressure}\ [kPa] - 58{,}31) * (-0{,}001278)
\end{aligned}
\tag{5}
$$

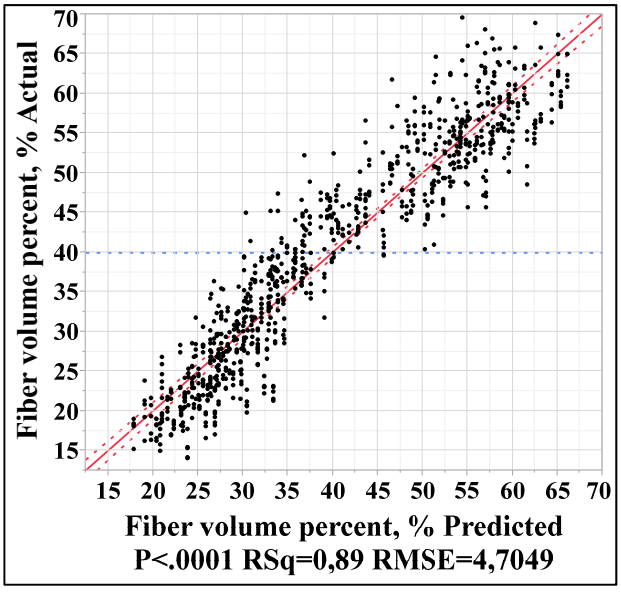

a

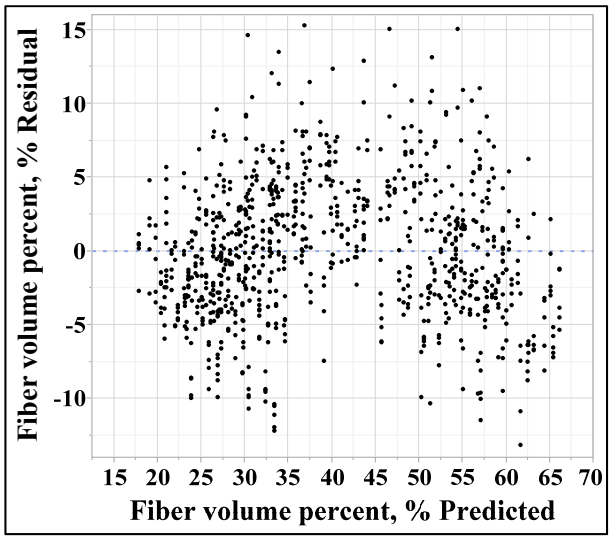

b

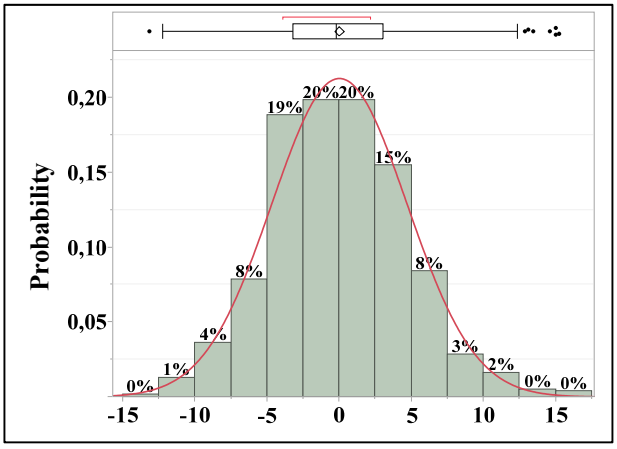

c

Figure 13. *Predicted versus actual (a), predicted versus residual (b), and the distribution of residual (c) fiber volume percents*

The prediction profilers given in Figure 14 reveal the effects of number of fabric layers, force type and pressure on the fiber volume percent of fabrics with different knit architecture. At all of the knit architecture levels, the other input variables exhibited the same effect on the fiber volume percent. The number of fabric layers increased the fiber volume percent and the 2-layer fabric stacks exhibited higher fiber volume percent than the 3-layer fabric stacks. Due to the hardening effect of the first compression, the fabrics showed a higher fiber volume percentage during the recovery period than the compression period. The relationship between pressure and fiber volume percent conforms to the power law model: for low pressures the curve increases perpendicularly and then it becomes a plateau for high pressures. The parallels observed in the interaction plots matrix indicated the lack of interactions between input variables (Figure 15). Figure 16 illustrates the effects of knit architecture, pressure, number of layer, and force type (compression or recovery period) on fiber volume percent in the form of 3D graphs.

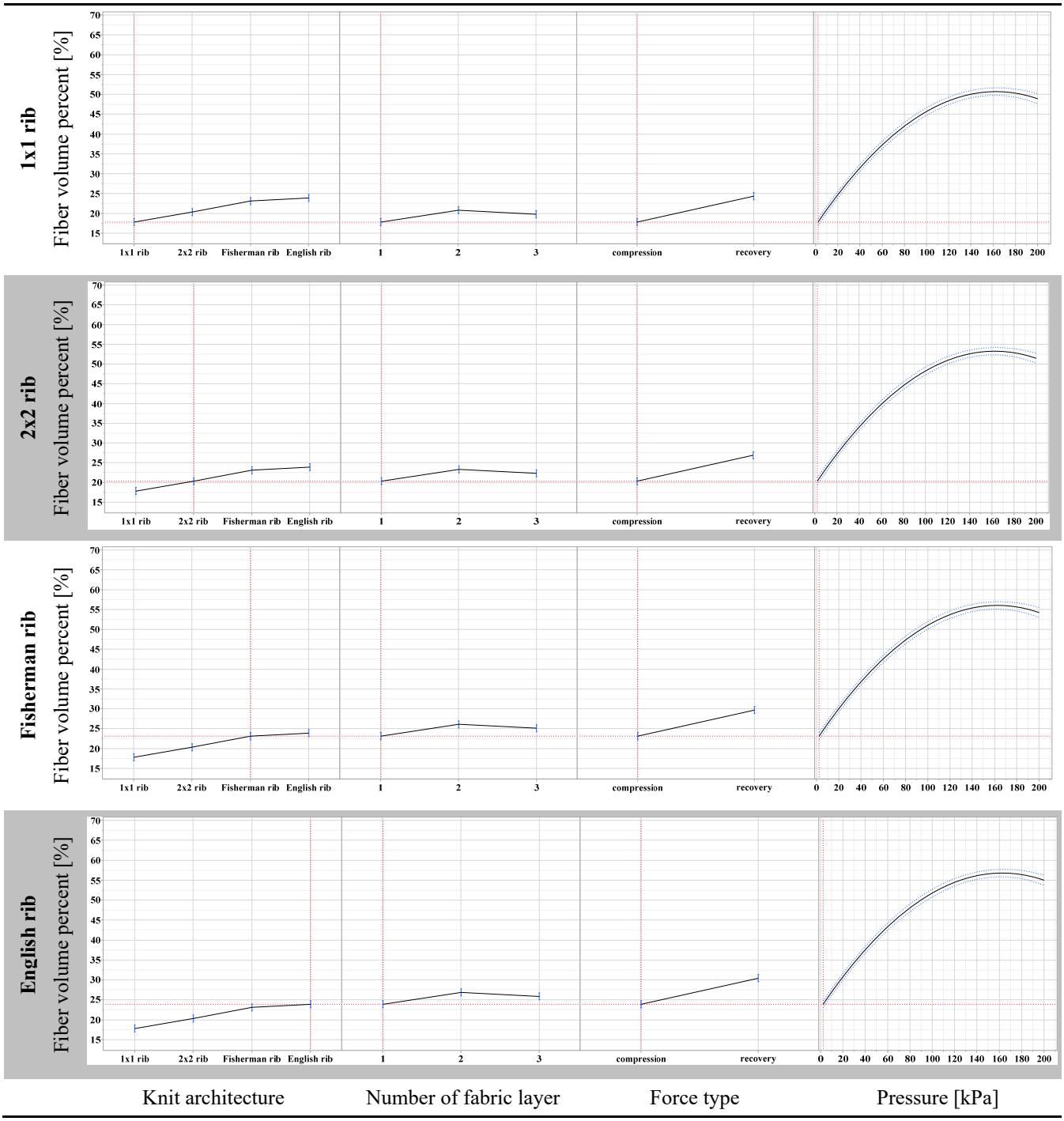

Figure 14. *The prediction profilers for fiber volume percent*

Note: The red vertical dashed line for each input variable on the horizontal axis indicates the current level of the input variable. The red horizontal dashed line indicates the fiber volume percent for the selected levels of the input variables. Continuous vertical error bar lines and the dashed lines showing the 95% confidence interval limits are blue.

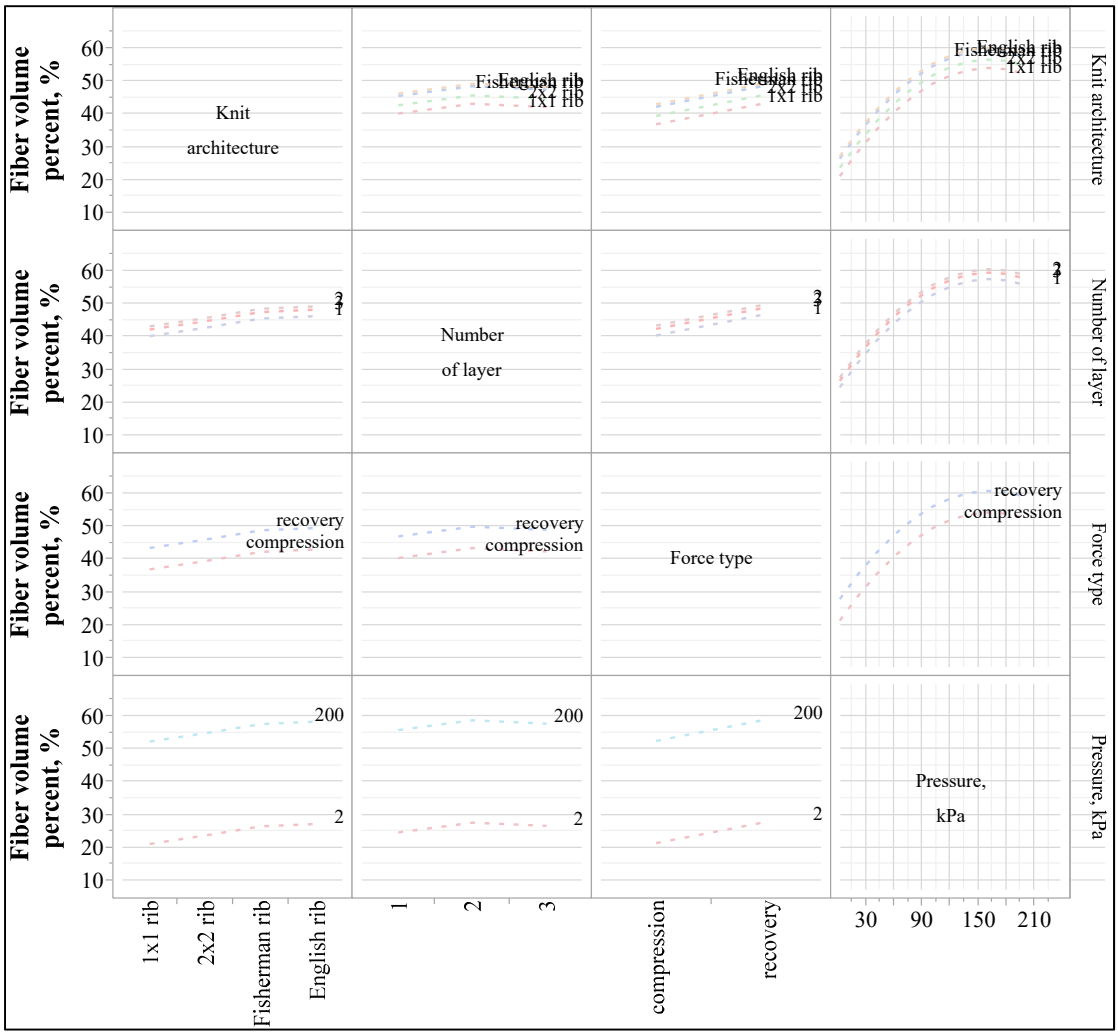

Figure 15. *Interaction plots matrix*

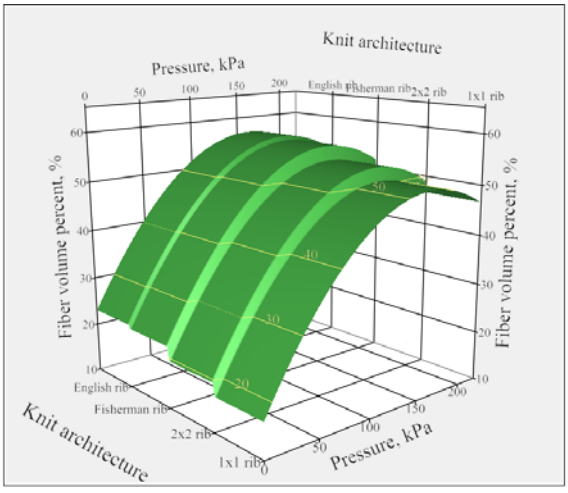

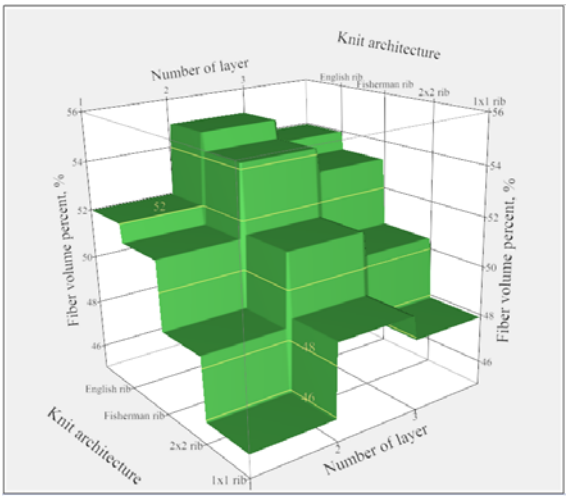

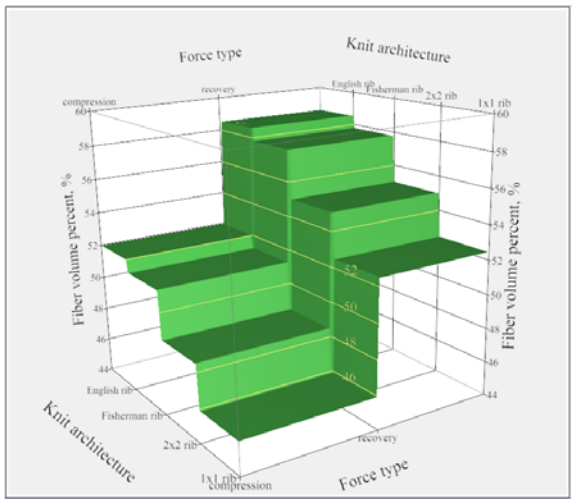

Figure 16. *Surface profilers for fiber volume percent*

4. Conclusion

In this study, weft knitted fabrics with 1x1, 2x2, English and fisherman rib architectures from glass yarn were produced and their structural and compressibility properties were analyzed in detail. The main findings of the single-layer fabric structural properties of the fabrics are:

i. The contractions in the width and/or length of the fabric, which vary in quantity depending on the knit architecture, control the structural properties of the fabric.

ii. While fabrics with 2x2 and fisherman rib knit architectures exhibited the highest thickness, the maximum fiber volume percent, the highest loop density and the shortest loop length; the fabric with 1x1 rib knit architecture displayed exactly the opposite of the relevant properties.

iii. These findings were related to the tendency of the fabric to shrink in the course direction for 2x2 rib knitted fabrics, while they were associated with the presence of tuck stitches for fisherman rib knitted fabrics.

Thereafter, the effects of knit architecture and the number of fabric layers on the compaction and relaxation behavior of the fabric stacks were discussed. The main findings of this discussion are:

i. The knit architecture affected the thickness and fiber content of single and multi-layer fabrics in the same trend.

ii. While a statistically non-significant negative association between the number of fabric layers and the normalized thickness (mm/layer) pointed out the beginning of the nesting; the number of fabric layers increased the fiber volume percent at a statistically significant level.

iii. The repeated compaction and relaxation processes reduced the thickness and increased the fiber volume percent.

iv. The power-law relationships with R^2s of greater than 0,90 between pressure and fiber volume percent were observed for both compaction and relaxation periods.

Acknowledgement

This work was supported by the Bilimsel Araştırma Projeleri (BAP) unit of Gaziantep University, Turkey under the grant number of MF.YLT.18.02.

References

[1]. Chawla K.K., Composite Materials: Science and Engineering. New York, Springer, 2019.

[2]. Mazumdar S.K., Composites manufacturing: materials, products, and process engineering. Boca Raton Fla, CRC Press, 2002.

[3]. Hammami A., Gebart B.R., "Analysis of the Vacuum Infusion Molding Process", Polymer Composites, 21, (2000), 28-40.

[4]. Correia N.C., Robitaille F., Long A.C., Rudd C.D., Simacek P., Advani S.G. "Use of Resin Transfer Molding Simulation to Predict Flow, Saturation, and Compaction in the VARTM Process", Journal of Fluids Engineering, 126, (2004), 210-215.

[5]. Govignon Q., Bickerton S., Morris J., Kelly P.A. "Full field monitoring of the resin flow and laminate properties during the resin infusion process", Composites Part A: Applied Science and Manufacturing, 39, (2008), 1412-1426.

[6]. Pearce N., Summerscales J., "The compressibility of a reinforcement fabric", Composites Manufacturing, 6, (1995), 15-21.

[7]. Lekakou C., Johari M.A.K.B., Bader M.G. "Compressibility and flow permeability of two-dimensional woven reinforcements in the processing of composites", Polymer Composites, 17, (1996), 666-672.

[8]. Robitaille F., Gauvin R., "Compaction of Textile Reinforcements for Composites Manufacturing. I: Review of Experimental Results", Polymer Composites", 19, (1998), 198-216.

[9]. Luo Y., Verpoest I., "Compressibility and Relaxation of a New Sandwich Textile Preform for Liquid

Composite Molding, Polymer Composites", 20, (1999), 179-191.

[10]. Potluri P., Sagar T.V., "Compaction modelling of textile preforms for composite structures", Composites Structures, 86, (2008), 177-185.

[11]. Lomov P., Molnár K., "Compressibility of carbon fabrics with needless electrospun PAN nanofibrous interleaves", Express Polymer Letters, 10, (2016), 25-35.

[12]. Yousaf Z., Potluri P., Withers P.J. "Influence of tow architecture on compaction and nesting in textile preforms", Applied Composite Materials, 24, (2017), 337-350.

[13]. Gommers B., Verpoest I., Van Houtte P. "Analysis of knitted fabric reinforced composites", Composites Part A: Applied Science and Manufacturing, 29, (1998), 1579-1588.

[14]. Pandita S.D., Falconet D., Verpoest I. "Impact properties of weft knitted fabric reinforced composites", Composite Science and Technology, 62, (2002), 1113-1123.

[15]. Pamuk G., Çeken F., "Manufacturing of Weft-Knitted Fabric Reinforced Composite Materials: A Review", Materials and Manufacturing Processes, 23, (2008), 635-640.

[16]. Ciobanu L., "Development of 3D Knitted Fabrics for Advanced Composite Materials", in Advances in Composite Materials – Ecodesign and Analysis, Edited by Brahim Attaf, InTech, 2011, pp. 161-192.

[17]. Marmaralı A.B., Atkı Örmeciliğine Giriş, İzmir, E.Ü Tekstil ve Konfeksiyon Araştırma – Uygulama Merkezi, 2004.

[18]. Marmaralı A., Kretzshmar S.D., Örme Terimleri ve Tanımlamaları, İzmir, E.Ü Tekstil ve Konfeksiyon Araştırma – Uygulama Merkezi, 2004.

[19]. Standard Test Methods for Mass per Unit Area (Weight) of Fabric, ASTM D3776, 2009.

[20]. Standard Test Methods for Wale and Course Count of Weft Knitted Fabrics, ASTM D8007, 2015.

[21]. British Standard Methods of test for Knitted Fabrics, BS 5441, 1998.

[22]. Statistical Software / JMP Software from SAS, 2021. [Online]. Available: https://www.jmp.com/en_us/home.html. [Accessed: May 27, 2021].

[23]. Kane C.D., Patil U.J., Sudhakar P. "Studies on the Influence of Knit Structure and Stitch Length on Ring and Compact Yarn Single Jersey Fabric Properties", Textile Research Journal, 77, (2007), 572-582.

[24]. Uyanık S., Değirmenci Z., Topalbekiroğlu M., Geyik F., "Examining the relation between the number and location of tuck stitches and bursting strength in circular knitted fabrics", Fibres & Textiles, 24, (2016), 114-119.

[25]. Uyanık S., Topalbekiroğlu M., "The effect of knit structures with tuck stitches on fabric properties and pilling resistance", The Journal of the Textile Institute, 108, (2017), 1584-1589.

[26]. İnce M.E., Yildirim H., "Air permeability and bursting strength of weft-knitted fabrics from glass yarn. Part II: knit architecture effect", The Journal of the Textile İnstitute, 110, (2019), 1072-1084..